Petroleum Science 19 (2022) 2460–2471

Contents lists available at ScienceDirect

Petroleum Science

journal homepage: www.keaipublishing.com/en/journals/petroleum-science

Original Paper

Adsorption behavior and wettability alteration of *bis*-imidazolium salts on vermiculite: Experimental and theoretical studies

Fan Ding, Tao Shen, Shan-Shan Mao, Xin Jin, Mang-Lai Gao*

State Key Laboratory of Heavy Oil Processing, College of Science, China University of Petroleum, Beijing, 102249, PR China

ARTICLE INFO

Article history:
Received 5 September 2021
Received in revised form
8 December 2021
Accepted 7 January 2022
Available online 19 January 2022

Edited by Xiu-Qiu Peng and Teng Zhu

Keywords:
Bis-imidazolium salts
Adsorption
Wettability alteration
Vermiculite
Molecular dynamics simulation

ABSTRACT

For further understanding the wettability alteration induced by organic salts, series of *bis*-imidazolium salts (EBMI, TBMI, HBMI, OBMI and DBMI) were employed for investigating their adsorption behavior and wettability alteration on vermiculite (Vt) by experimental and theoretical studies. The characterization results indicated that all *bis*-imidazolium salts had been loaded on Vts. The adsorption results showed that EBMI, TBMI, HBMI, OBMI and DBMI on Vt reached equilibrium of 0.159, 0.156, 0.145, 0.114 and 0.084 mmol g^{-1} around 30 min at 25 °C, respectively, which were sensitive to ionic strength and pH. Langmuir, statistical physical modelling and pseudo-second-order models could be well fitted with the adsorption data, and thermodynamic parameters suggested that the adsorption processes of *bis*-imidazolium salts were endothermic and spontaneous, indicating that the resultant *bis*-imidazolium salts could be self-assembled onto Vt in the form of the monolayer. Results of molecular dynamic simulation showed that *bis*-imidazolium salts were adsorbed on Vt with the lying-flat configuration, and the electrostatic interaction acted as the main interaction mechanism, which were consistent with that obtained experimentally. Changes of wettability of Vt induced by *bis*-imidazolium salts were verified by capillary rise experiments. Interestingly, the wettability of organo-Vts varied with the spacer length and the order was as follows: EBMI-Vt < TBMI-Vt < HBMI-Vt < OBMI-Vt < DBMI-Vt, which could be explained by their arrangements, hydrophobicity as well as the interaction energies. The longer the spacers of *bis*-imidazolium salts, the greater the absolute values of the interaction energy, the less the adsorbed *bis*-imidazolium salts, while the more hydrophobic of organo-Vt. This work aimed at revealing the adsorption behavior, mechanism as well as effect of *bis*-imidazolium salts on wettability alteration of negatively charged mineral surface, providing some information for the selection of flooding agent for enhanced oil recovery and wettability modifier.

1. Introduction

With the development course of economy, the energy problem has been focused, and petroleum, a conventional but indispensable source of energy, still plays an essential role in our daily life, which requests more efficiently methods for boosting recovery (Madani et al., 2019). During the process of oil production, reservoir wettability and its alteration works as one of imperative mechanisms of enhanced displacement efficiency (Gao et al., 2019; Purswani and Karpyn, 2019; Ding and Gao, 2021; Eltoum et al., 2021; Sun et al., 2021). For understanding the knowledgement of wettability, which not only EOR, but also acts as an important mechanism in water purification (Tang et al., 2021; Yu et al., 2021; Zhang et al., 2021), attempts have been carried out, and the surfactant displays can favorable capacity for changing the wettability, which affects by their types and structures (Jarrahian et al., 2012; Hou et al., 2015; Ding et al., 2018b).

Ahmadi and Shadizadeh (2013, 2015) have studied the adsorption characteristics of surfactant originated from Zizyphus Spina Christi on the carbonate and sandstone, of which the adsorption data can be well fitted by Freundlich. The contact angle results indicate that the wettability of reservoir can be altered to more water-wetness. Zhou et al. (2020) have synthesized series of synthesized piperazine-based polyether gemini surfactants and investigated their adsorption on the montmorillonite, and the results show that both of the wettability and adsorption of

* Corresponding author.
E-mail address: mlgao@cup.edu.cn (M.-L. Gao).

https://doi.org/10.1016/j.petsci.2022.01.009

surfactants varies with the alkyl chain increasing. Based on the wettability changes with the surfactant adsorption as well as their structures, however, the underlying correlation among those three is still blurred, and studies on how the organic salts with smaller and simpler structures affect the wettability are still not comprehensive both from the experiment and theoretical perspectives. For an in-depth comprehension of wettability alteration induced by organic molecules, molecular dynamics (MD) simulation that combined with experiment as an effectively method and give rise to the insight into the relationship between surfactant adsorption and wettability alteration at microscopic level (Liu et al., 2020).

Concerns about the demands of industry development and environment protection have been increased over years, the greener and friendlier surfactant is urgent to be developed. Imidazolium-based surfactants have been focused as a potential alternative by the reason of their favorable biodegradability, low toxicity and innocuousness in human health (Kamboj et al., 2012; Xiang et al., 2019b). Velusamy et al. (2017) have indicated the synergistic effect of imidazolium-based ionic liquids on interfacial tension and wettability alteration. Ao et al. (2009) have comparatively investigated the aggregation behavior and wettability of imidazolium gemini surfactant and its monomer on silicon wafer, which affects by their structures. Xiang et al. (2019a) have synthesized a series of imidazolium-based gemini surfactants with the long alkyl chain for modifying clay minerals, and the results show that all of modified clays tend to be more hydrophobic. Even though there are several literatures on the wettability of imidazolium surfactant, systematic studies on the wettability altered by *bis*-imidazolium salts with short alkyl chain as well as the mechanism are seldom reported, which may endow some new insights both on the wettability alteration and other applications.

Additionally, layer charge, one of intrinsic character, also has effect on the surface properties of mineral (Koutsopoulou et al., 2020). As the negatively charge of surface provide binding sites, it may alter the arrangement and adsorbed number of surfactants, thereby, change the wettability (Pazos et al., 2012; Ishiguro and Koopal, 2016). Luo et al. (2014a, 2014b) have reported the wettability alteration of montmorillonites that own relatively low layer charge. In fact, there is as yet no comprehensive understanding of how the adsorption and wettability of surfactant alters on high layer charge surface.

In this work, vermiculite (Vt) with high layer charge was chose as matrix, and series of *bis*-imidazolium salts with different spacers were employed for exploring their adsorption characteristics and wettability alteration. The intercalation and microstructure of *bis*-imidazolium salts in vermiculite were characterized by X-ray diffraction (XRD), scanning electron microscope (SEM), fourier transformed infrared spectroscopy (FT-IR), and thermogravimetric-differential thermogravimetric analysis (TG-DTG). The adsorption experiments of the synthesized *bis*-imidazolium salts on the vermiculite were proceeded at different concentration of surfactant solution, contact times, temperatures, ionic strengths and pH, and their adsorption isotherms, kinetics, as well as thermodynamics were explored detailly. The MD simulation was conducted to validate the adsorption configurations of *bis*-imidazolium salts, and the adsorption energies were calculated to clarify their adsorption characteristics and wettability alteration. And the wettability alteration was tested by capillary rise experiments with Lipophilic to Hydrophilic Ratio (*LHR*) values. This work aims at exploring the adsorption behavior, mechanism and wettability alteration of *bis*-imidazolium salts on highly charged surface, providing certain new sight of understanding and theoretical guidance not only on the oilfield exploitation, but also on the organic modification of the clay mineral.

2. Materials and methods

2.1. Materials

The raw Vt supplied by Sigma-Aldrich was chosen as the matrix for exploring the surfactants adsorption behavior on negatively charged clay. Reagents utilized in synthesis of *bis*-imidazolium salts, 1-methylimidazole, 1,2-dibromoethane, 1,4-dibromobutane, 1,6-dibromohexane, 1,8-dibromooctane, 1,10-dibromodecane, isopropanol and ethyl acetate, were provided by J&K, Aladdin and Energy Chemical, respectively. NaCl and $CaCl_2$, HCl and NaOH used for separately adjusting ionic strength and pH were purchased from the Beijing Chemical Works. Cyclohexane obtained from Energy Chemical and deionized water (18 MΩ cm) were served as the oil and water phases in capillary rise experiments.

2.2. Synthesis of bis-imidazolium salts

The *bis*-imidazolium salts were synthesized in the accordance with literatures (Baltazar et al., 2007; Zhang et al., 2018), of which the synthetic route and structures were shown in Fig. 1. Briefly, 1-methylimidazole (0.2 mol) and dibromo alkane ($Br(CH_2)_nBr$ (n = 2, 4, 6, 8, 10), 0.1 mol) were mixed with isopropanol (20 mL) in the round-bottom flask. After heated to reflux for 24 h and cooled, the mixture was washed by ethyl acetate for three times to get rid of the impurities, and the resultant was gathered by extraction filtration and dried in the vacuum oven for 48 h. The resulting products, ethylene *bis*-(1-methylimidazoline) dibromide, tetramethylene *bis*-(1-methylimidazoline) dibromide, hexamethylene *bis*-(1-methylimidazoline) dibromide, octamethylene *bis*-(1-methylimidazoline) dibromide, decamethylene *bis*-(1-methylimidazoline) dibromide were named as EBMI, TBMI, HBMI, OBMI, and DBMI, respectively. All resultant surfactants were characterized by ^1H NMR, elemental analysis and fourier transformed infrared spectroscopy (FT-IR).

2.3. Adsorption experiments

Batch adsorption experiments of *bis*-imidazolium salts on the pristine Vt were proceed with the following operation processes: 0.3 g of Vt was put in 30 mL of surfactant solution in the water bath oscillator at 200 rpm for a certain time. After high-speed centrifugation, the concentration of residual *bis*-imidazolium salts in supernatant was detected at 224 nm through UV–Vis, and the amounts q_e (mmol g^{-1}) of *bis*-imidazolium salts adsorbed on Vt could be calculated by Eq. (1). The precipitates were collected and dried at 80 °C overnight, then sifted by 200 mush sieves for further clarifying the wettability alteration that induced by intercalation of *bis*-imidazolium salts in Vt. The obtained organo-vermiculites (organo-Vts) were labeled as EBMI-Vt, TBMI-Vt, HBMI-Vt, OBMI-Vt, and OBMI-Vt, separately.

$$q_e = \frac{C_0 - C_e}{m} \cdot V \tag{1}$$

where C_0 (mmol L^{-1}) and C_e (mmol L^{-1}) represent the initial and equilibrium concentrations of *bis*-imidazolium salts solution correspondingly. m (g) means the dosage of Vt, and V (L) is the volume of solution. The effects of concentration of *bis*-imidazolium salts (0.62, 1.23, 1.85, 2.46, 3.69 and 4.92 mmol L^{-1}, which the dosage of surfactants corresponding to 0.05, 0.1, 0.15, 0.2, 0.3 and 0.4 CEC of 0.5 g Vt in 50 mL solution, respectively), contact time (1, 5, 10, 15, 20, 30, 60, 120, and 180 min), temperature (25, 40 and 60 °C), ionic strength of Na^+ and Ca^{2+} (1 and 2 mol L^{-1}) and pH (2,

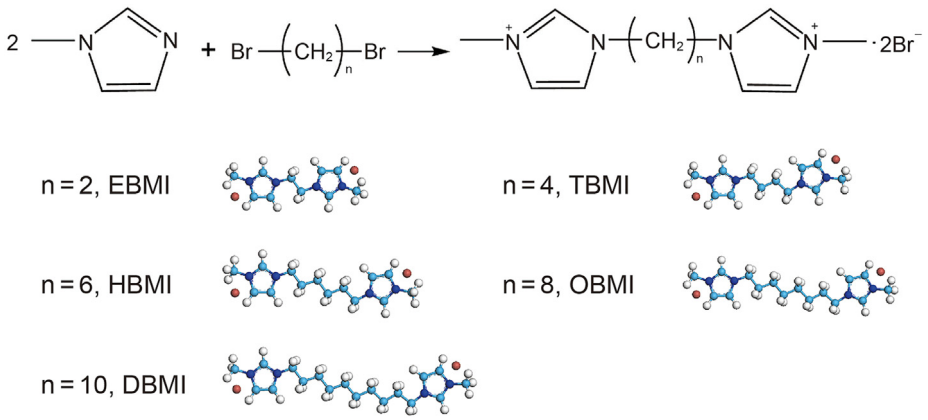

Fig. 1. Schematic diagram of synthetic route and the structures of *bis*-imidazolium salts.

4, 6, 8, 10) were carried out, and adsorption isotherms, kinetics, thermodynamics as well as statistical physical modelling were employed for elucidating the adsorption processes, which calculating details were listed in Supporting materials.

Meanwhile, for the sake of understand the relationship of *bis*-imidazolium salts adsorption and wettability alteration, MD simulation is employed for verifying the adsorption processes and configuration of *bis*-imidazolium salts on Vts in microscopic level.

2.4. Characterizations

FT-IR of surfactants (EBMI, TBMI, HBMI, OBMI, and DBMI), Vt and organo-Vts were performed by FT-IR spectrometer (Nicolet iS10) in KBr pellets, in which the scanning range of 4000–400 cm^{-1} and the resolution of 4 cm^{-1}. Thermogravimetric analyses (TG) of the particles were conducted via TG-DSC3+ STARe system (Mettler Toledo) at nitrogen atmosphere. The X-ray diffraction (XRD) patterns of the raw and obtained organo-Vts were scanned and recorded at the range of 2–10° by X-ray diffractometer (Bruker D8 Advance) with Cu Kα radiation at 40 kV and 40 mA, and the layer spacing of the samples could be calculated by $\lambda = 2d \sin\theta$. The morphology of particles was collected by scanning electron microscope (SEM, SU8010, Japan).

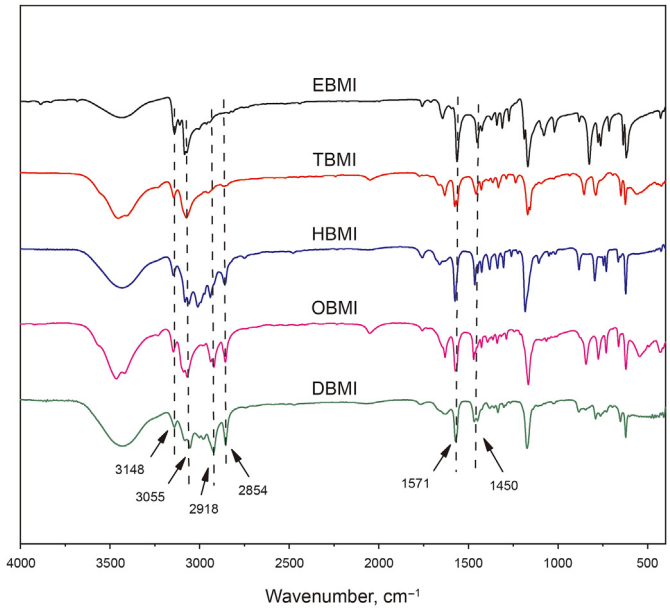

Fig. 2. FT-IR spectra of synthesized *bis*-imidazolium salts.

2.5. Capillary rise experiment

The wetting properties of organo-Vts were appraised through capillary rise experiments, which was suitable to measure the wettability of heterogeneity of the real mineral surface (Chau, 2009). After the sample was put into Washburn tubes and compacted, it went to test the wettability by cyclohexane and deionized water. Once the liquid contacted the bottom of the particles, it rose in the packed powder bed through capillary pressure, and the wettability could be obtained. The data were recorded and the value of Lipophilic to Hydrophilic Ratio (*LHR*) that described the wetting properties were calculated by the following equations (Ding et al., 2018b):

$$LHR = 2.772 \cdot \frac{k_o}{k_w} \quad (2)$$

where *LHR* represents the relative wettability of sample, k_o (kPa^2 s^{-1}) and k_w (kPa^2 s^{-1}) are wetting rates towards oil and water phases, respectively, which are obtained by the plots of $(\Delta P)^2$ versus *t*.

3. Results and discussion

3.1. Characterizations

3.1.1. Characterizations of bis-imidazolium salts

FT-IR spectra of synthesized *bis*-imidazolium salts are shown in Fig. 2. The peaks of the surfactants appeared at 3055 cm^{-1} with a small shoulder at 3148 cm^{-1} are ascribed as the vibrations of =C–H (Wang et al., 2014a, 2014b). Bands at 2918 and 2854 cm^{-1} are due to the C–H symmetrical and asymmetrical stretching vibrations of *bis*-imidazolium salts, and the tiny but sharped IR adsorption bands at 1450 cm^{-1} correspond to their C–H asymmetrical bending vibrations (Pillai et al., 2018; Sharma et al., 2020; Pillai and Mandal, 2022). The characteristic pointed bands at 1571 cm^{-1} are attributed to the stretching vibrations of imidazole rings (Pillai et al., 2017, 2018). ^1H NMR and element analysis data of the resultant surfactants are listed in Table 1. Results of these characterizations indicate that the synthetic products are target *bis*-imidazolium salts that own the higher purity.

Table 1
Elemental analysis and ^{1}H NMR of series of *bis*-imidazolium salts.

	Elemental analysis						^{1}H NMR
	C, %		H, %		N, %		
	Cal.	Exp.	Cal.	Exp.	Cal.	Exp.	
EBMI	34.09	32.72	4.55	4.66	15.91	15.28	δ 8.93 (s, 2H), 7.62 (s, 2H), 7.53 (s, 2H), 4.89 (s, 4H), 4.01 (s, 6H)
TBMI	37.89	37.74	5.26	5.09	14.74	14.49	δ 8.81 (s, 2H), 7.55 (s, 2H), 7.49 (s, 2H), 4.31 (t, 4H), 3.94 (s, 6H), 1.97 (m, 4H)
HBMI	41.16	41.15	5.88	5.88	13.72	13.49	δ 8.72 (s, 2H), 7.47 (s, 2H), 7.43 (s, 2H), 4.19 (t, 4H), 3.88 (s, 6H), 1.88 (m, 4H), 1.34 (m, 4H)
OBMI	44.04	41.38	6.42	6.64	12.84	12.27	δ 8.84 (s, 2H), 7.59 (s, 2H), 7.53 (s, 2H), 4.26 (t, 4H), 3.97 (s, 6H), 1.91 (m, 4H), 1.35 (s, 8H)
DBMI	46.55	45.49	6.90	6.83	12.07	11.86	δ 8.85 (s, 2H), 7.57 (s, 2H), 7.51 (s, 2H), 4.24 (t, 4H), 3.94 (s, 6H), 1.88 (m, 4H), 1.29 (m, 12H)

3.1.2. FT-IR and TG-DTG analyses of organo-vermiculites

The results of FT-IR of original Vt and organo-Vts are exhibited in Fig. 3a. The broad and strong bands around 3415 cm^{-1} are resulted from the stretching vibration of structural hydroxyl and adsorbed water of the clay particles (Ding et al., 2018a), and the small but shaped bands at 1649 cm^{-1} are owing to the H–O–H bending vibration of adsorbed water (Luo et al., 2017a; Ding et al., 2018a). The extra weak bands near to 3159 and 3095, 2932 and 2857, as well as 1467 cm^{-1} of organo-Vts are attributed to the vibrations of = C–H and C–H of *bis*-imidazolium salts, respectively (Lazorenko et al., 2018; Pillai et al., 2018; Sharma et al., 2020). The most feature bands at 1568 cm^{-1} are assigned to the stretching vibrations of the imidazole rings (Luo et al., 2017a; Pillai et al., 2018), suggesting that the series of *bis*-imidazolium salts have been introduced or adsorbed onto Vt (Zhou et al., 2009).

Fig. 3b shows the curves of TG-DTG analyses of the Vt and organo-Vts. Seen from the Fig. 3b, the additional peaks at around 441.8 °C are related to the decomposition of *bis*-imidazolium salts of organo-Vts (Luo et al., 2017a; Ding et al., 2018a). These disparities in weight losses between organo-Vt and original one indicates that the *bis*-imidazolium salts have been intercalated into the Vts, which is mutually corroborated with the FT-IR results. Moreover, as the peaks around 50–200 °C of Vt may be caused by the water in the particle (Su et al., 2016; Luo et al., 2017b; Ding et al., 2018a), the discrepancy between pristine and organo-Vt at the weight loss peaks at the range of 50–200 °C manifest that the *bis*-imidazolium salts adsorption turns the particle to be less water-wetness (Su et al., 2016; Ding et al., 2018b).

3.1.3. XRD analysis of organo-vermiculites

The intercalation of *bis*-imidazolium salts on the Vts are detected by XRD, of which the patterns are depicted in Fig. 4. The peak at about 6.2° is related to the characteristic basal spacing of 1.43 nm of Vt, and the oblate peak at around 7.4° with the *d*-value of 1.18 nm is related to hydration phase in Vt (Yin et al., 2017). After introduced the surfactants, a minor displacement of the most peaks of organo-Vts can be spotted, of which the basal spacings are around 1.42 nm, indicating that all surfactants insert into the layers of Vt with the monolayer arrangement (Ding et al., 2018b). It is worth noting that the *d*-spacing of the organo-Vts enlarges from 1.41 nm to 1.43 nm with the length of spacer increasing, which may be attributed to the increasing size of inserted *bis*-imidazolium salts (Wu et al., 2015). Moreover, the facts that interlayer distances of the organo-Vts move from 1.14 nm to 1.16/1.17 nm also have proved the intercalation of surfactant.

In general, as the positively charged *bis*-imidazolium salts are adsorbed and interposed into the interlayers to offset part of electrostatic repulsion between the negatively charged layers of Vt, a slightly decrease of layer spacing could be occurred, while the size of surfactant actually also has effect on the *d*-spacings of organo-Vts. Even that, all of these *bis*-imidazolium salts in Vts adopt a monolayer arrangement that accords with the results obtained by

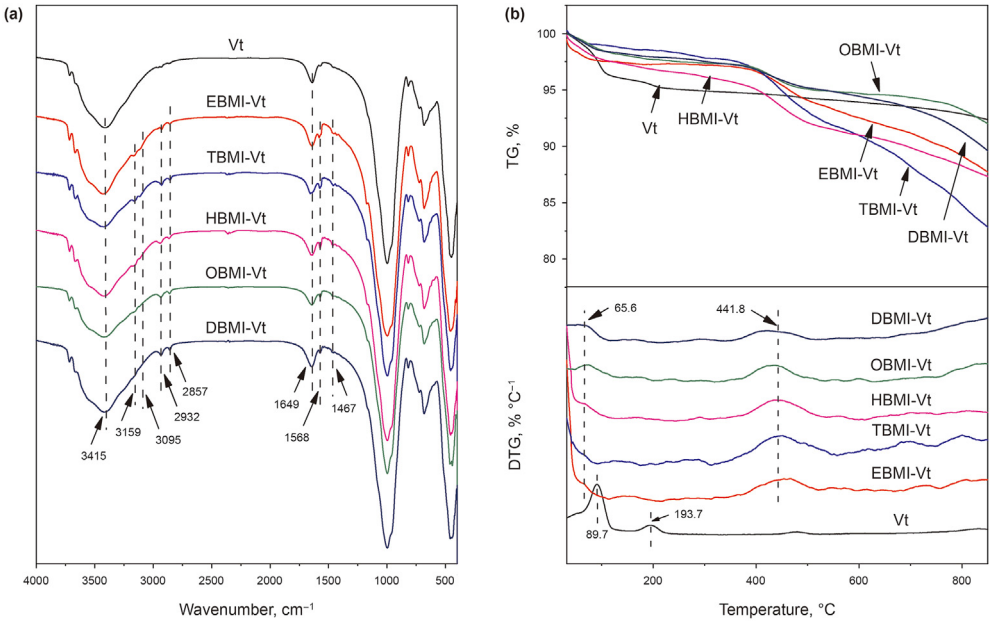

Fig. 3. The FT-IR spectra (a) and TG-DTG curves (b) of Vt and organo-Vts.

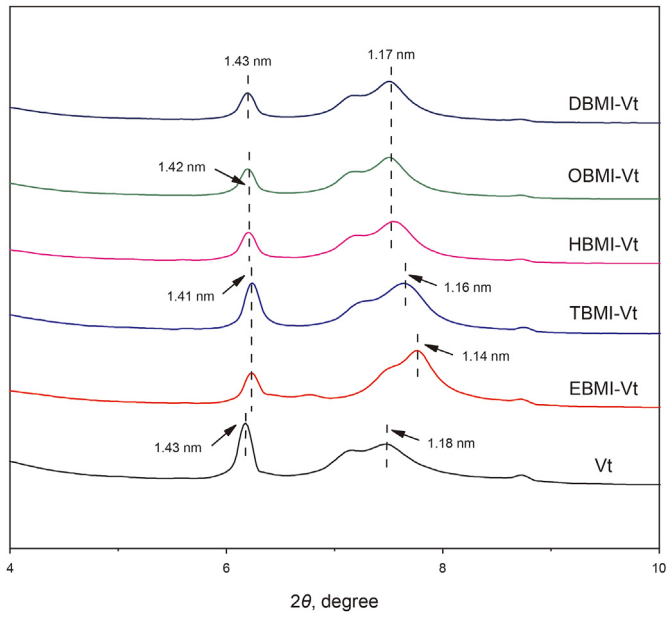

Fig. 4. The XRD patterns of Vt and organo-Vts.

adsorption isotherm and MD simulation, which proves that the reliability of the simulation results.

3.1.4. Morphology analysis of organo-vermiculites

The microtopography of the raw Vt and organo-Vts is characterized by SEM, which is shown in Fig. 5. All of the Vt and its derivates own the stratified structure. Differently, the raw Vt exhibits a typical laminated structure of silicate with fluffy surface (Fig. 5a), while other organo-Vts display the tight packed lamellar textures (Fig. 5b–f). These morphology changes may be due to the intercalation/adsorption of surfactants into the interlayer of the Vt.

3.2. Adsorption behavior of bis-imidazolium salts

3.2.1. Effects of concentration, time and temperature

Fig. 6a–c depict the influences of concentration, time and temperature on the adsorption of *bis*-imidazolium salts on Vt, respectively. Seen from the Fig. 6a, with the augment of concentration of *bis*-imidazolium salts, the adsorption amount of EBMI, TBMI, HBMI, OBMI, and DBMI on Vts increase gradually and reach saturation at 0.159, 0.156, 0.145, 0.114 and 0.084 mmol g^{-1}, respectively, which shows an opposite sequence of the increasing length of spacer of these *bis*-imidazolium salts. Based on the difference of size between surfactants, the negatively charged sites of Vt are covered by the longer spacer of surfactant, and the electrostatic interaction between the surface and *bis*-imidazolium salts is weaken, leading to the reduction in the adsorption (Pillai and Mandal, 2019).

The influence of time on *bis*-imidazolium salts adsorption are presented in Fig. 6b. With the time elapsing, the adsorption amount of EBMI, TBMI, HBMI, OBMI, and DBMI rises and achieve equilibrium at around 30 min. On the basis of this fact, these *bis*-imidazolium salts show a characteristic of relatively quick adsorption behavior on Vt, which may give the credit to their simpler and relatively small structures that easily access the interlayers of Vt and adsorb onto the surface (Ding et al., 2018a).

The adsorption amount of Vt toward *bis*-imidazolium salts at different temperature is displayed in Fig. 6c. As the temperature raises from the 25, 40–60 °C, the q_e of EBMI on Vt reveals a gradually growth from the 0.154, 0.161–0.168 mmol g^{-1}, and the same increasing trends are found in the adsorption of TBMI (from 0.152, 0.159–0.167 mmol g^{-1}), HBMI (from 0.143, 0.153–0.162 mmol g^{-1}), OBMI (from 0.112, 0.121, to 0.131 mmol g^{-1}), and DBMI (from 0.082, 0.096–0.107 mmol g^{-1}), indicating that the temperature is conducive to these adsorption processes. Notably, though the temperature influences all surfactant absorbed on Vts, the sequence of the adsorption amount of these surfactants still keep as follows: EBMI > TBMI > HBMI > OBMI > DBMI. That is to say, for

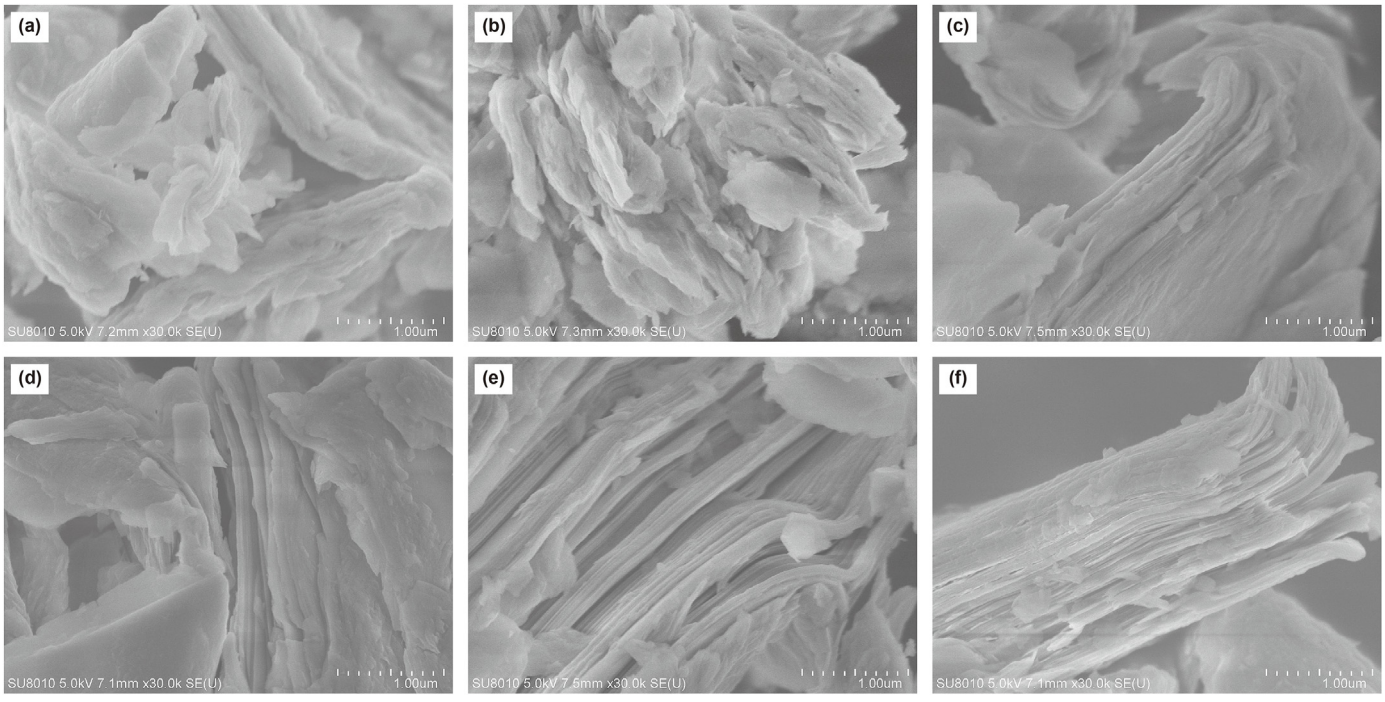

Fig. 5. The SEM images of Vt (a), EBMI-Vt (b), TBMI-Vt (c), HBMI-Vt (d), OBMI-Vt (e) and DBMI-Vt (f).

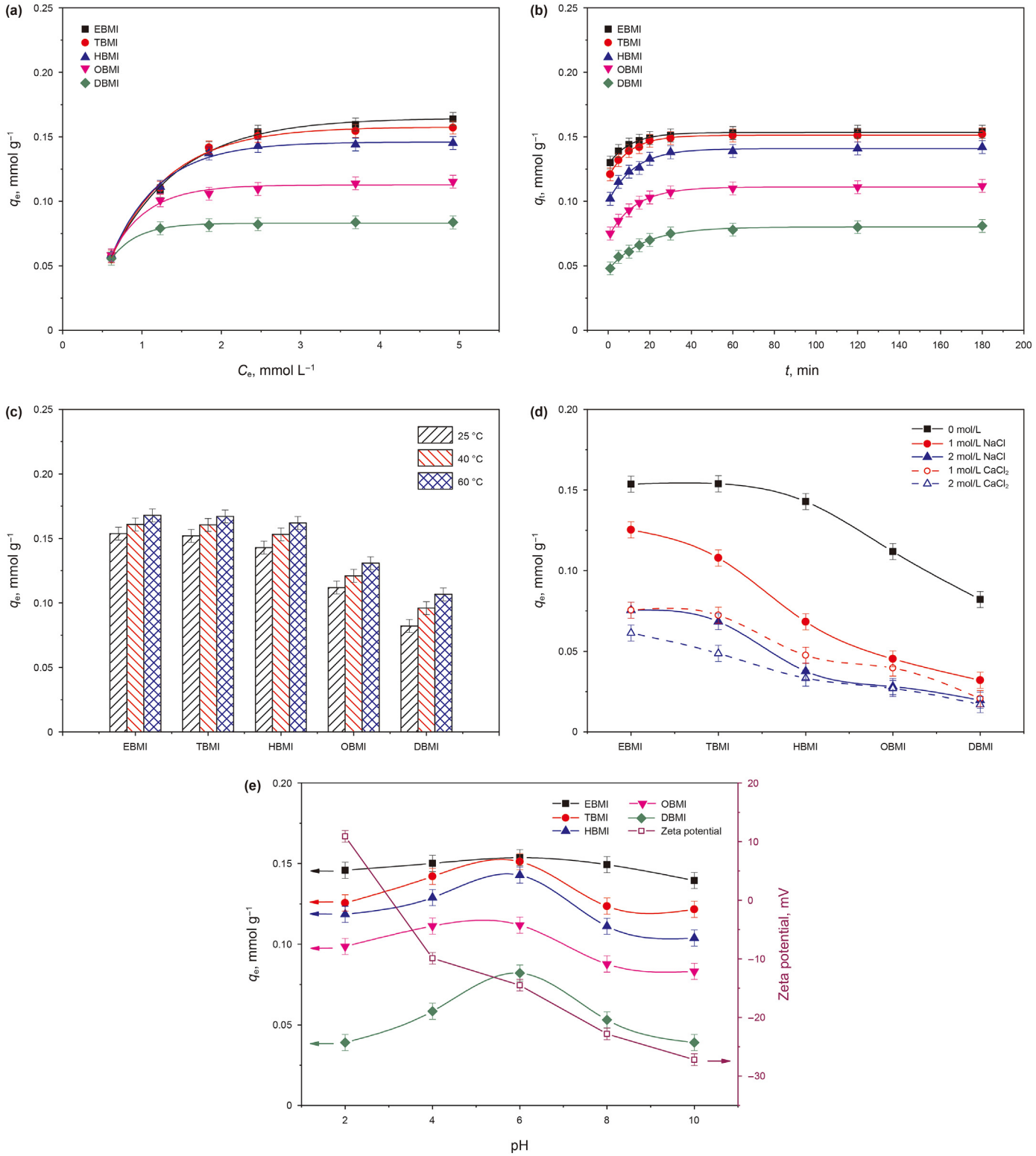

Fig. 6. The effects of concentration (a), contact time (b), temperature (c), ion strength (d) and pH (e) on the adsorption behavior of *bis*-imidazolium salts on Vts, respectively.

these series of *bis*-imidazolium salts, the length of spacer, which may result in the steric hindrance, exhibit a side-effect on their adsorption.

3.2.2. Effects of ionic strength and pH

The influences of ionic strength and pH on the *bis*-imidazolium salts adsorption are shown in Fig. 6d–e, respectively. As the concentration of the inorganic ions (Na^+/Ca^{2+}) augments from 0, 1–2 mol L^{-1}, the adsorption amount of the resulting EBMI declines precipitously from the 0.154, 0.125/0.076 to 0.076/0.061 mmol L^{-1}, and others exhibit similar tendencies. All of surfactants adsorption processes are sensitive to the ionic strength, and this phenomenon can be responsible for these cationic ions that interact with the negatively charged surface, and reduce the effective binding sites of Vts, therefore, leading to the decrease of surfactants adsorbed (Zeng et al., 2018). Additionally, the inhibiting effect of Ca^{2+} on surfactant adsorption are higher than Na^+, which may be attributed to their differential valence state.

As depicted in Fig. 6e, the amounts of surfactants adsorbed on Vts vary with the change of pH. Based on the Zeta potential of Vt reduces with the pH increasing, when the pH < 6, the q_e of the resulting surfactants gradually increase with the pH increasing, resulting by the intensified electrostatic interaction of *bis*-imidazolium salts with negatively charged surface of Vt (Gürses et al., 2009). As the pH higher than 6, the surface charge of Vt turns to more negative, but the adsorption amounts of surfactant downdrift which possibly due to (i) the existence of the Na^+ and/or (ii) the surfactant molecules that keep the neutral state that have weakened interaction between surfactant and Vt during adsorption in the solution (Wu et al., 2014). Both of the two factors verified that electrostatic interaction plays as the major driving force for the adsorption of these resulting *bis*-imidazolium salts onto Vts (Pillai and Mandal, 2019).

3.2.3. Isotherms, kinetics and thermodynamics

For further probing the adsorption characteristics and processes of EBMI, TBMI, HBMI, OBMI, and DBMI on Vts, their adsorption isotherms, kinetics and thermodynamics have been studied, and the results are putted in Fig. 7a–c and Tables 2–4. For adsorption isotherms, the data are well matched by Langmuir (Fig. 7a) than Freundlich models (not shown), of which the fitting regression coefficients (R^2) of the former are all greater than 0.98, indicating that the adsorption of EBMI, TBMI, HBMI, OBMI, and DBMI on Vts are monolayer adsorption which has no interaction between the adsorbed *bis*-imidazolium salts (Xin et al., 2011; Yuan et al., 2015; Pillai and Mandal, 2019). This consequence maybe due to their extremely short alkyl chains that are insufficient to form the hydrophobic interaction between molecules. Furthermore, good correlations ($R^2 > 0.98$) between the statistical physical modelling and adsorption data were obtained and tabulated in Table 2, and the parameters of n of this model are all around unity, which meaning almost one binding site of Vt interact with one cationic head group of molecules only by electrostatic interaction (Shamsudin et al., 2020). The values of D_m (from 0.199 to 0.083, corresponding to from EBMI to DBMI) indicate that the density of the binding sites of Vts decreases as the surfactant spacer increases, which further bear out the size of surfactant molecule may be counterproductive in their adsorption and confirm the aforementioned conjecture of the changes in the adsorption of resultant surfactants on Vts.

The fitting results of the two classical kinetic models, pseudo-first- and pseudo-second-order models, are shown in Fig. 7b and Table 3. According to kinetic parameters listed in Table 3, the coefficients of pseudo-second-order ($R^2 = 0.999$) are larger than that of pseudo-first-order ($R^2 < 0.921$), and the values of q_e calculated by pseudo-second-order are closer to the experimental values than the former one. Both of these two aspects prove that the adsorption processes of EBMI, TBMI, HBMI, OBMI, and DBMI are well abided with the pseudo-second-order kinetic model. In addition, the rate indexes ($k_2 q_e$) of pseudo-second-order model of *bis*-imidazolium salts adsorption are also ranked with the order of EBMI > TBMI > HBMI > OBMI > DBMI, which may be resulted from the structure of the surfactant molecules (Guo et al., 2020).

Fig. 7c and Table 4 display the results of adsorption thermodynamics of synthesized *bis*-imidazolium salts on Vts. As tabulated in Table 4, the ΔH° and ΔS° values of all adsorption processes are positive, while the ΔG° values are negative, confirming that these adsorptions of EBMI, TBMI, HBMI, OBMI, and DBMI on Vts are endothermic, increased randomness and spontaneous processes (Bhatti et al., 2017; Shen et al., 2020). Moreover, the absolute value of ΔG° that increases with temperature also suggest the affinity of these surfactants to Vt is promoted by higher temperature (Chowdhury et al., 2011).

In conclusion, once the Vt is putted into these synthesized *bis*-imidazolium salts solutions, there is the monolayer organic phase of these imidazolium-based surfactants can be rapidly self-assembled on Vts by electrostatic interaction, which are sensitive to the ionic strength, pH as well as temperature.

3.3. Molecular dynamics simulation

The MD simulation is conducted using the MS software. The supercell of Vt ($4 \times 4 \times 1$) is established according the prototype reported by Gruner (1934), and the adsorption configurations of EBMI, HBMI and DBMI on Vts are chose as representatives and portrayed in Fig. 8. As seem from Fig. 8a and d, the two imidazole rings of EBMI are parallel to the surface and the whole molecular is lied onto the surface. HBMI and DBMI also display the similar simulation results. These interesting facts may be attributed to their special structures of *bis*-imidazolium salts, which own two rigid cationic imidazolium rings, that can be absorbed on the negatively charged surface of vermiculite through electrostatic interaction (Xie et al., 2020). With the spacer length increasing, the distances between *bis*-imidazolium salts and surface gradually increase from 0.2709, 0.3124 and 0.3161 nm. Moreover, the configurations of adsorbed *bis*-imidazolium salts come to curved, which covers more surface area (Fig. 8e–f), may result in more tightly arrangement of *bis*-imidazolium salts betwixt layers and more hydrophobic surface.

The interaction energy of series of *bis*-imidazolium salts on Vts has been calculated by the following Eq. (3) (Rai et al., 2011) and tabulated in Table 5.

$$\Delta E = E_{sys} - E_1 - E_2 \tag{3}$$

where ΔE represents interaction energy of *bis*-imidazolium salt on Vt, and E_{sys}, E_1 and E_2 mean the energies of adsorption system, vermiculite surface and *bis*-imidazolium salt, respectively. As tabulated in Table 5, the negative interaction energies of *bis*-imidazolium salts indicate that their adsorption on Vt is spontaneous (Lyu et al., 2018), which matches with the experimental results. And the absolute values of interaction energies of *bis*-imidazolium salts increase from 138.58 to 144.96 kcal mol^{-1} with the spacer length increasing. The greater absolute value of energy, the more favorable interaction between *bis*-imidazolium salt and surface, the more stable structure of surfactant adsorbed on Vt (Rai et al., 2011; Ouachtak et al., 2021). Thereby, it can be inferred that DBMI can form a stabilized organic monolayer, resulting in the more hydrophobic surface of Vt. Moreover, as the proportion of electrostatic energy of *bis*-imidazolium salts take much larger than that of van der Waals, the electrostatic interaction plays the vital role in the

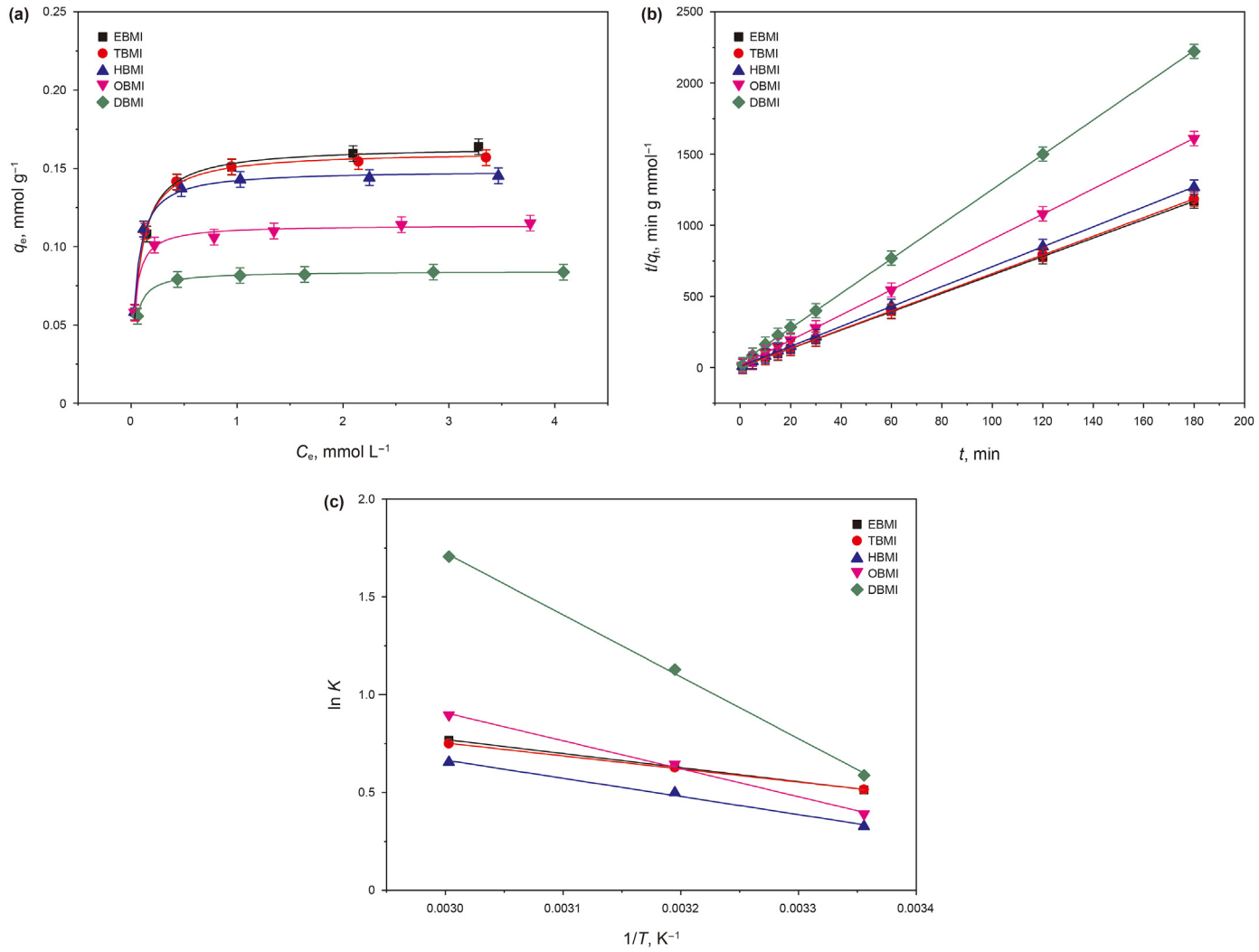

Fig. 7. The plots of the data fitted by Langmuir model (a), pseudo-second-order model (b), as well as the plot of ln$K$ versus 1/T (c) for the adsorption of *bis*-imidazolium salts on Vts, respectively.

Table 2
Isotherm parameters of *bis*-imidazolium salts on Vts ($V = 30$ mL, Adsorbent mass = 0.3 g, $T = 25$ °C).

	Langmuir			Freundlich			Statistical physics modelling		
	q_{max}, mmol g^{-1}	K_L, L mmol^{-1}	R^2	K_F, mmol$^{1-(1/n)}$ L$^{1/n}$ g^{-1}	n_F	R^2	n	D_m	R^2
EBMI	0.164	14.335	0.993	0.143	5.759	0.844	0.853	0.199	0.998
TBMI	0.160	15.640	0.996	0.140	6.173	0.794	0.937	0.172	0.996
HBMI	0.149	19.523	0.996	0.132	6.912	0.751	0.997	0.149	0.994
OBMI	0.114	32.460	0.988	0.104	8.772	0.786	0.946	0.121	0.985
DBMI	0.084	32.646	0.999	0.078	11.702	0.780	1.010	0.083	0.998

Table 3
Kinetic parameters for adsorption of *bis*-imidazolium salts on Vts ($C_0 = 0.246$ mmol L^{-1}, $V = 30$ mL, Adsorbent mass = 0.3 g, $T = 25$ °C).

	Pesudo-first-order			Pesudo-second-order			
	q_e, mmol g^{-1}	k_1, min^{-1}	R^2	q_e, mmol g^{-1}	k_2, g (mmol min)$^{-1}$	$k_2\, q_e$, min^{-1}	R^2
EBMI	0.013	0.031	0.912	0.154	9.882	1.522	0.999
TBMI	0.013	0.020	0.775	0.152	8.705	1.323	0.999
HBMI	0.021	0.023	0.891	0.143	5.246	0.750	0.999
OBMI	0.020	0.027	0.921	0.113	5.497	0.621	0.999
DBMI	0.021	0.019	0.894	0.082	4.469	0.366	0.999

Table 4
Thermodynamic parameters for the adsorption of *bis*-imidazolium salts on Vts (for EBMI, TBMI, and HBMI, $C_0 = 2.46$ mmol L^{-1}, for OBMI, $C_0 = 1.845$ mmol L^{-1}, for DBMI, $C_0 = 1.23$ mmol L^{-1}, $V = 30$ mL, Adsorbent mass = 0.3 g).

	ΔH°, kJ mol^{-1}	ΔS°, J mol^{-1} K^{-1}	ΔG°, kJ mol^{-1}		
			$T = 298$ K	$T = 313$ K	$T = 333$ K
EBMI	5.977	24.339	−1.276	−1.641	−2.128
TBMI	5.550	22.913	−1.278	−1.622	−2.080
HBMI	7.712	28.665	−0.830	−1.260	−1.834
OBMI	11.890	43.213	−0.987	−1.636	−2.500
DBMI	26.304	93.246	−1.483	−2.882	−4.747

interaction between the organic molecules and vermiculite surface (Wu et al., 2015).

3.4. Wettability alteration of organo-vermiculites

3.4.1. Capillary rise experiment

The wettability of the resulting organo-Vts is evaluated through Washburn capillary rise experiments, and the obtained wetting rates and the calculated values of *LHR* are listed in Table 6. After the *bis*-imidazolium salts inserted into the Vt, the value of k_o increases from 0.066 to >0.331, and that of k_w ranges from 0.142 to >0.207. Significantly, the improvement of k_o is larger than that of k_w, manifesting that the organo-Vts are of a stronger affinity for oil phase. Moreover, compared with the original Vt, the organo-Vts show the greater *LHR* values (>4.21). Considering that the higher the value of *LHR* than unity, the more hydrophobic of the material (Susana et al., 2012), all of these organo-Vts, by contrast, own the more lyophobicity. This alteration may be resulted by the intercalation of the surfactants into the Vt layers, which formed the monolayer organic phase.

Table 6
The average values of k_o, k_w and *LHR* of organo-Vts.

	Vt	EBMI-Vt	TBMI-Vt	HBMI-Vt	OBMI-Vt	DBMI-Vt
k_o, kPa^2 s^{-1}	0.066	0.331	0.370	0.357	0.381	0.450
k_w, kPa^2 s^{-1}	0.142	0.218	0.228	0.213	0.207	0.212
LHR	1.29	4.21	4.50	4.65	5.10	5.88

The wettability of Vt has not only affected by the interposition of *bis*-imidazolium salts, but also varies with the chain length of spacer of *bis*-imidazolium salts. As the spacer length increases, the wettability of organo-Vts changes with the following order: EBMI-

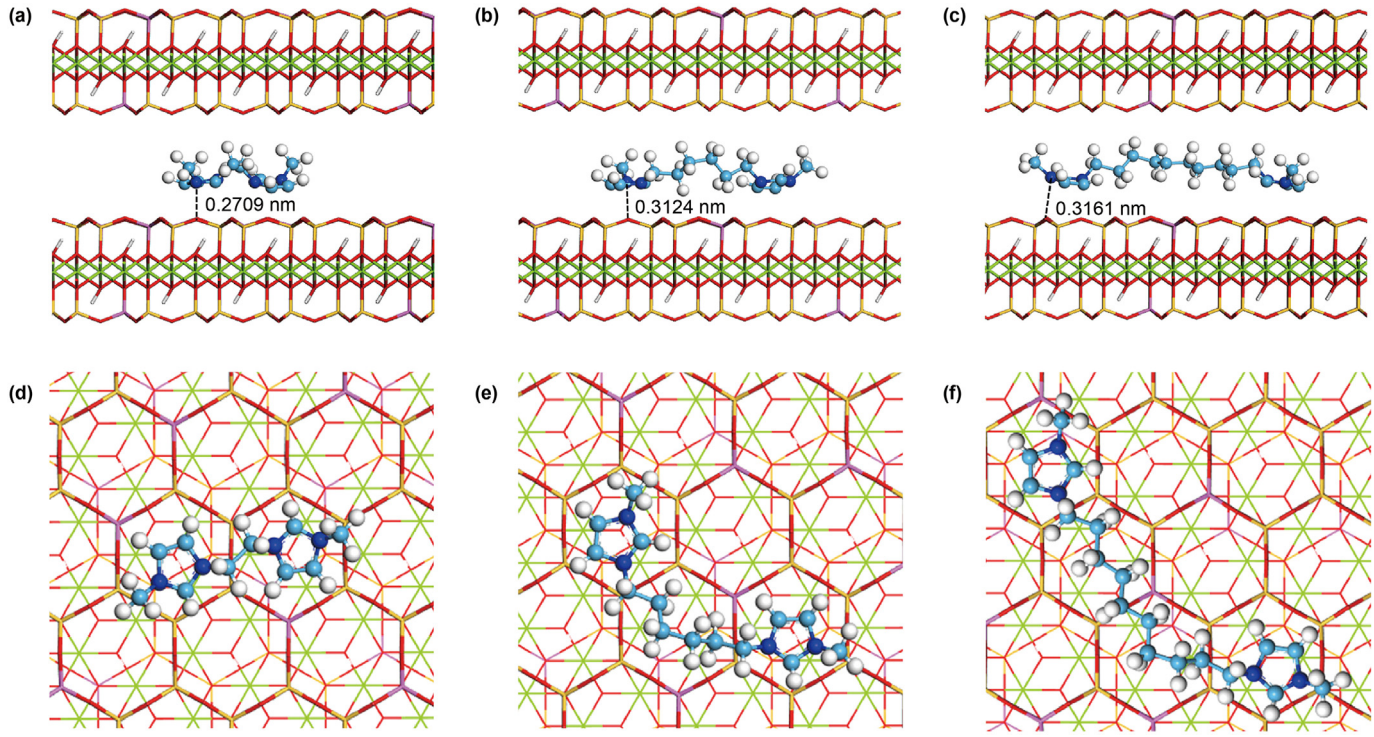

Fig. 8. The adsorption configurations of EBMI (a, d), HBMI (b, e) and DBMI (c, f) on Vts in the front and vertical views, respectively.

Table 5
The interaction, electrostatic and van der Waals energies of series of *bis*-imidazolium salts with Vts.

	Interaction energy, kcal mol^{-1}	Electrostatic energy, kcal mol^{-1}	Van der Waals energy, kcal mol^{-1}
EBMI	−138.58	−123.74	−14.28
TBMI	−140.26	−122.07	−17.57
HBMI	−140.27	−120.35	−19.21
OBMI	−140.84	−119.85	−20.20
DBMI	−144.96	−117.96	−26.12

Vt < TBMI-Vt < HBMI-Vt < OBMI-Vt < DBMI-Vt, which is antithetical to the sequence of the adsorption amount of these surfactants on Vts. This result presumably due to (i) the arrangements of the *bis*-imidazolium salts inserted on Vt, (ii) the hydrophobicity of *bis*-imidazolium salts themselves induced by their structures (Paria and Khilar, 2004), (iii) the interaction energies of *bis*-imidazolium salts adsorbed on Vts.

3.4.2. Wettability alteration

Given that their similar structures, the EBMI, HBMI and DBMI, which own different length spacer, are chosen as the templates and discussed the wettability alteration that combined with the results of characterization, adsorption and MD simulation. In view of the arrangements of interposed *bis*-imidazolium salts on Vts, there is an organic monolayer self-assembled on the interlayer surface of Vt by electrostatic interaction, which is shown in Fig. 9. The EBMI with shorter spacer may array in a relatively discrete way, while the DBMI with the longer spacer probably shows a more tightly monolayer arrangement. It can be assumed that the sites of Vt that can bind organic molecule keep constant, as the spacer length of *bis*-imidazolium salts increases, the binding sites and surface of Vt are covered, therefore, the adsorbed surfactants decrease but compactly arrange in the interlayers of Vts, resulting in the enhancement of the hydrophobicity of Vt (Ding et al., 2018b). In case of the properties of molecule itself, the order of hydrophobicity of organo-Vts is accordance with the length of spacer of surfactants, it may be explained by the enhanced oil affinity of surfactant with the increasing spacer length (Wu et al., 2015). Finally, in perspective of interaction energy of *bis*-imidazolium salts with Vt surface, as seen from the Table 5, the interaction between DBMI and surface shows the higher absolute value of energy than others, indicating that DBMI forms a more stabilized organic layer which results in a more hydrophobic surface of Vt.

By reason of the foregoing, the wettability alteration of these imidazolium-based organo-Vts has been controlled by the structure as well as the arrangement of the surfactant, in which the structure may take the pivotal role. The longer spacer of *bis*-imidazolium salts, the larger interaction between those and vermiculite, the more hydrophobicity of organo-Vts.

4. Conclusion

Inspired by the kindly environmental properties and unique structures of imidazole derivatives, series of *bis*-imidazolium salts with higher purity are synthesized and characterized by FT-IR, EA and ^{1}H NMR. The characterization results indicate that all *bis*-imidazolium salts have been intercalated into the vermiculites. And the adsorption behavior of these synthetic surfactants on Vts have been investigated detailly, and the results show that the adsorption of *bis*-imidazolium salts (EBMI, TBMI, HBMI, OBMI and DBMI) reached equilibrium at 0.159, 0.156, 0.145, 0.114 and 0.084 mmol g^{-1} around 30 min at 25 °C, which are also sensitive to ionic strength and pH, indicating that the adsorption is affected by the structure of *bis*-imidazolium salts and electrostatic interaction. Adsorption data are well agreed with Langmuir, statistical physical modelling and pseudo-second-order models, and the calculated thermodynamic parameters confirm that the adsorption are endothermic and spontaneous processes, indicating that the resulting *bis*-imidazolium salts can be self-assembled onto Vts in the form of monolayers. MD simulation results verify that *bis*-imidazolium salts are adsorbed in the interlamination of Vt with the flat-lying adsorption configuration, and the electrostatic interaction acts as the main interaction mechanism, which is accordance with the results found experimentally. As the capillary rise experiments results shows, the wettability of organo-Vts is altered with *bis*-imidazolium salts. The hydrophobicity of Vt and organo-Vts is increasing in the order of Vt < EBMI-Vt < TBMI-Vt < HBMI-Vt < OBMI-Vt < DBMI-Vt. Combined with the results of adsorption, molecular simulation and wetting tests, this interesting fact can be explained by (i) the arrangement of *bis*-imidazolium salts; (ii) the increased lipophilicity of longer spacer-containing surfactant itself; (iii) the interaction energy of *bis*-imidazolium salts. The longer the spacers of *bis*-imidazolium salts, the greater the interaction energy, the less the adsorbed *bis*-imidazolium salts, while the more hydrophobic of organo-Vt. This work tries to illustrate the adsorption behavior and mechanism of *bis*-imidazolium salts on Vts and their wettability alteration by experimentally and theoretically, providing some enlightenments for the molecular design of organic wetting modifier and flooding agent for EOR.

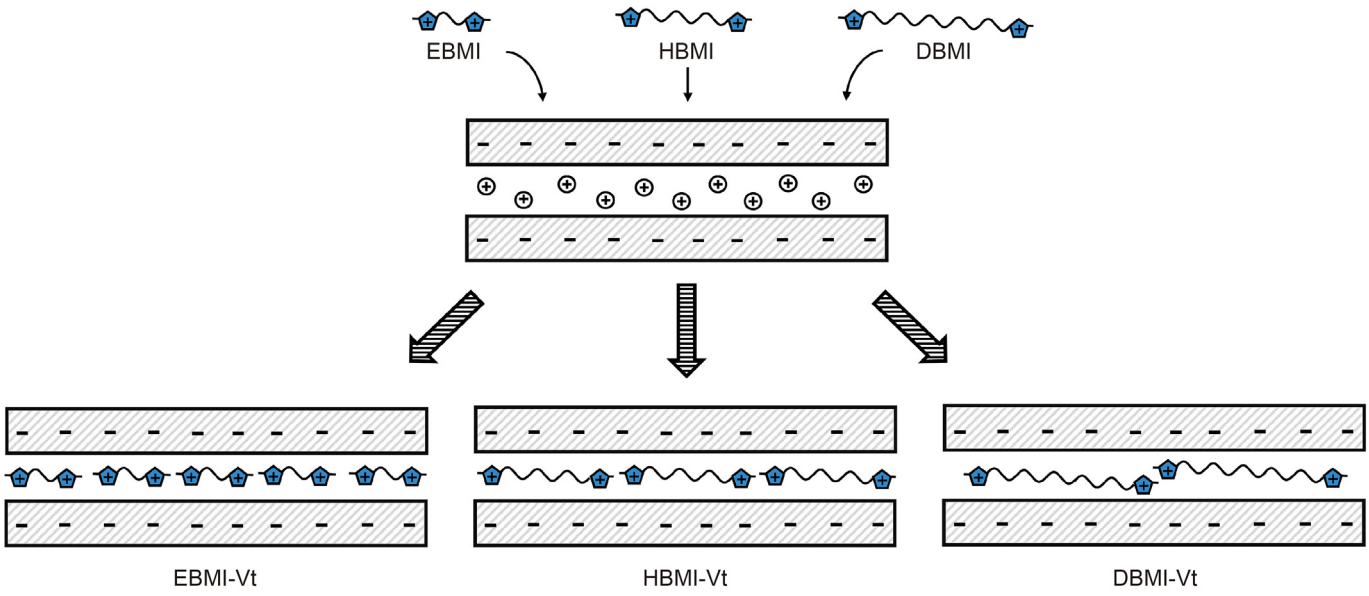

Fig. 9. Schematic diagram of the arrangements of EBIM, HBMI and DBMI in the interlamination of Vts, respectively.

Acknowledgement

This work is funded by the National Natural Science Foundation of China [Grant No. 21776306].

Appendix A. Supplementary data

Supplementary data to this article can be found online at https://doi.org/10.1016/j.petsci.2022.01.009.

References

Ahmadi, M.A., Shadizadeh, S.R., 2013. Experimental investigation of adsorption of a new nonionic surfactant on carbonate minerals. Fuel 104, 462–467. https://doi.org/10.1016/j.fuel.2012.07.039.

Ahmadi, M.A., Shadizadeh, S.R., 2015. Experimental investigation of a natural surfactant adsorption on shale-sandstone reservoir rocks: static and dynamic conditions. Fuel 159, 15–26. https://doi.org/10.1016/j.fuel.2015.06.035.

Ao, M., Xu, G., Pang, J., et al., 2009. Comparison of aggregation behaviors between Ionic liquid-type imidazolium gemini surfactant [C_{12}-4-C_{12}im]Br_2 and its monomer [C_{12}mim]Br on silicon wafer. Langmuir 25 (17), 9721–9727. https://doi.org/10.1021/la901005v.

Baltazar, Q.Q., Chandawalla, J., Sawyer, K., et al., 2007. Interfacial and micellar properties of imidazolium-based monocationic and dicationic ionic liquids. Colloids Surf. A Physicochem. Eng. Asp. 302 (1–3), 150–156. https://doi.org/10.1016/j.colsurfa.2007.02.012.

Bhatti, H.N., Jabeen, A., Iqbal, M., et al., 2017. Adsorptive behavior of rice bran-based composites for malachite green dye: isotherm, kinetic and thermodynamic studies. J. Mol. Liq. 237, 322–333. https://doi.org/10.1016/j.molliq.2017.04.033.

Chau, T.T., 2009. A review of techniques for measurement of contact angles and their applicability on mineral surfaces. Miner. Eng. 22 (3), 213–219. https://doi.org/10.1016/j.mineng.2008.07.009.

Chowdhury, S., Mishra, R., Saha, P., et al., 2011. Adsorption thermodynamics, kinetics and isosteric heat of adsorption of malachite green onto chemically modified rice husk. Desalination 265 (1–3), 159–168. https://doi.org/10.1016/j.desal.2010.07.047.

Ding, F., Gao, M.L., 2021. Pore wettability for enhanced oil recovery, contaminant adsorption and oil/water separation: a review. Adv. Colloid Interface Sci. 289, 102377. https://doi.org/10.1016/j.cis.2021.102377.

Ding, F., Gao, M.L., Shen, T., et al., 2018a. Comparative study of organo-vermiculite, organo-montmorillonite and organo-silica nanosheets functionalized by an ether-spacer-containing Gemini surfactant: Congo red adsorption and wettability. Chem. Eng. J. 349, 388–396. https://doi.org/10.1016/j.cej.2018.05.095.

Ding, F., Gao, M.L., Wang, J., et al., 2018b. Tuning wettability by controlling the layer charge and structure of organo-vermiculites. J. Ind. Eng. Chem. 57, 304–312. https://doi.org/10.1016/j.jiec.2017.08.037.

Eltoum, H., Yang, Y., Hou, J., 2021. The effect of nanoparticles on reservoir wettability alteration: a critical review. Petrol. Sci. 18 (1), 136–153. https://doi.org/10.1007/s12182-020-00496-0.

Gao, M.L., Gu, Z., Luo, Z.X., 2019. One-layer-only molecular deposition filming flooding: a review. Colloids Surf. A Physicochem. Eng. Asp. 572, 182–196. https://doi.org/10.1016/j.colsurfa.2019.04.009.

Gruner, J.W., 1934. The structures of vermiculites and their collapse by dehydration. Am. Mineral. 19 (12), 557–575.

Guo, S.X., Gao, M.L., Shen, T., 2020. Dipyridyl-based organo-silica nanosheets for three emerging micropollutants efficient removal: adsorption performance and mechanisms. J. Clean. Prod. 260, 121149. https://doi.org/10.1016/j.jclepro.2020.121149.

Gürses, A., Karaca, S., Açikyildiz, M., et al., 2009. Thermodynamics and mechanism of cetyltrimethylammonium adsorption onto clayey soil from aqueous solutions. Chem. Eng. J. 147 (2–3), 194–201. https://doi.org/10.1016/j.cej.2008.07.001.

Hou, B., Wang, Y., Huang, Y., 2015. Mechanistic study of wettability alteration of oil-wet sandstone surface using different surfactants. Appl. Surf. Sci. 330, 56–64. https://doi.org/10.1016/j.apsusc.2014.12.185.

Ishiguro, M., Koopal, L.K., 2016. Surfactant adsorption to soil components and soils. Adv. Colloid Interface Sci. 231, 59–102. https://doi.org/10.1016/j.cis.2016.01.006.

Jarrahian, K., Seiedi, O., Sheykhan, M., et al., 2012. Wettability alteration of carbonate rocks by surfactants: a mechanistic study. Colloids Surf. A Physicochem. Eng. Asp. 410, 1–10. https://doi.org/10.1016/j.colsurfa.2012.06.007.

Kamboj, R., Singh, S., Bhadani, A., et al., 2012. Gemini imidazolium surfactants: synthesis and their biophysiochemical study. Langmuir 28 (33), 11969–11978. https://doi.org/10.1021/la300920p.

Koutsopoulou, E., Koutselas, I., Christidis, G.E., et al., 2020. Effect of layer charge and charge distribution on the formation of chitosan-smectite bionanocomposites. Appl. Clay Sci. 190, 105583. https://doi.org/10.1016/j.clay.2020.105583.

Lazorenko, G., Kasprzhitskii, A., Yavna, V., 2018. Synthesis and structural characterization of betaine- and imidazoline-based organoclays. Chem. Phys. Lett. 692, 264–270. https://doi.org/10.1016/j.cplett.2017.12.054.

Liu, Z., Zhou, G., Li, S., et al., 2020. Molecular dynamics simulation and experimental characterization of anionic surfactant: influence on wettability of low-rank coal. Fuel 279, 118323. https://doi.org/10.1016/j.fuel.2020.118323.

Luo, Z., Pei, J., Wang, L., et al., 2017a. Influence of an ionic liquid on rheological and filtration properties of water-based drilling fluids at high temperatures. Appl. Clay Sci. 136, 96–102. https://doi.org/10.1016/j.clay.2016.11.015.

Luo, Z., Wang, L., Yu, P., et al., 2017b. Experimental study on the application of an ionic liquid as a shale inhibitor and inhibitive mechanism. Appl. Clay Sci. 150, 267–274. https://doi.org/10.1016/j.clay.2017.09.038.

Luo, Z.X., Gao, M.L., Gu, Z., et al., 2014a. Structures and wettability alterations of a series of bispyridinium dibromides exchanged with reduced-charge montmorillonites. Energy Fuel. 28 (9), 6163–6171. https://doi.org/10.1021/ef5011385.

Luo, Z.X., Gao, M.L., Ye, Y.G., et al., 2014b. Wettability studies of reduced-charge montmorillonites modified by quaternary ammonium salts using capillary rise test. Powder Technol. 266, 167–174. https://doi.org/10.1016/j.powtec.2014.06.023.

Lyu, X., You, X., He, M., et al., 2018. Adsorption and molecular dynamics simulations of nonionic surfactant on the low rank coal surface. Fuel 211, 529–534. https://doi.org/10.1016/j.fuel.2017.09.091.

Madani, M., Zargar, G., Takassi, M.A., et al., 2019. Fundamental investigation of an environmentally-friendly surfactant agent for chemical enhanced oil recovery. Fuel 238, 186–197. https://doi.org/10.1016/j.fuel.2018.10.105.

Ouachtak, H., El Guerdaoui, A., Haounati, R., et al., 2021. Highly efficient and fast batch adsorption of orange G dye from polluted water using superb organo-montmorillonite: experimental study and molecular dynamics investigation. J. Mol. Liq. 335, 116560. https://doi.org/10.1016/j.molliq.2021.116560.

Paria, S., Khilar, K.C., 2004. A review on experimental studies of surfactant adsorption at the hydrophilic solid–water interface. Adv. Colloid Interface Sci. 110 (3), 75–95. https://doi.org/10.1016/j.cis.2004.03.001.

Pazos, M.C., Castro, M.A., Orta, M.M., et al., 2012. Synthetic high-charge organomica: effect of the layer charge and alkyl chain length on the structure of the adsorbed surfactants. Langmuir 28 (19), 7325–7332. https://doi.org/10.1021/la300153e.

Pillai, P., Kumar, A., Mandal, A., 2018. Mechanistic studies of enhanced oil recovery by imidazolium-based ionic liquids as novel surfactants. J. Ind. Eng. Chem. 63, 262–274. https://doi.org/10.1016/j.jiec.2018.02.024.

Pillai, P., Mandal, A., 2019. Wettability modification and adsorption characteristics of imidazole-based ionic liquid on carbonate rock: implications for enhanced oil recovery. Energy Fuel. 33 (2), 727–738. https://doi.org/10.1021/acs.energyfuels.8b03376.

Pillai, P., Mandal, A., 2022. Synthesis and characterization of surface-active ionic liquids for their potential application in enhanced oil recovery. J. Mol. Liq. 345, 117900. https://doi.org/10.1016/j.molliq.2021.117900.

Pillai, P., Pal, N., Mandal, A., 2017. Synthesis, characterization, surface properties and micellization behaviour of imidazolium-based ionic liquids. J. Surfactants Deterg. 20 (6), 1321–1335. https://doi.org/10.1007/s11743-017-2021-1.

Purswani, P., Karpyn, Z.T., 2019. Laboratory investigation of chemical mechanisms driving oil recovery from oil-wet carbonate rocks. Fuel 235, 406–415. https://doi.org/10.1016/j.fuel.2018.07.078.

Rai, B., Sathish, P., Tanwar, J., et al., 2011. A molecular dynamics study of the interaction of oleate and dodecylammonium chloride surfactants with complex aluminosilicate minerals. J. Colloid Interface Sci. 362 (2), 510–516. https://doi.org/10.1016/j.jcis.2011.06.069.

Shamsudin, M.S., Azha, S.F., Sellaoui, L., et al., 2020. Fabrication and characterization of a thin coated adsorbent for antibiotic and analgesic adsorption: experimental investigation and statistical physical modelling. Chem. Eng. J. 401, 126007. https://doi.org/10.1016/j.cej.2020.126007.

Sharma, V., Bhatia, C., Singh, M., et al., 2020. Synthesis, thermal stability and surface activity of imidazolium monomeric surfactants. J. Mol. Liq. 308, 113006. https://doi.org/10.1016/j.molliq.2020.113006.

Shen, T., Wang, L., Zhao, Q., et al., 2020. Single and simultaneous adsorption of basic dyes by novel organo-vermiculite: a combined experimental and theoretical study. Colloids Surf. A Physicochem. Eng. Asp. 601, 125059. https://doi.org/10.1016/j.colsurfa.2020.125059.

Su, X., Ma, L., Wei, J., et al., 2016. Structure and thermal stability of organo-vermiculite. Appl. Clay Sci. 132–133, 261–266. https://doi.org/10.1016/j.clay.2016.06.011.

Sun, Y., Xin, Y., Lyu, F., et al., 2021. Experimental study on the mechanism of adsorption-improved imbibition in oil-wet tight sandstone by a nonionic surfactant for enhanced oil recovery. Petrol. Sci. 18, 1115–1126. https://doi.org/10.1016/j.petsci.2021.07.005.

Susana, L., Campaci, F., Santomaso, A.C., 2012. Wettability of mineral and metallic powders: applicability and limitations of sessile drop method and Washburn's technique. Powder Technol. 226, 68–77. https://doi.org/10.1016/j.powtec.2012.04.016.

Tang, H., Wang, J., Zhang, S., et al., 2021. Recent advances in nanoscale zero-valent iron-based materials: characteristics, environmental remediation and challenges. J. Clean. Prod. 319, 128641. https://doi.org/10.1016/j.jclepro.2021.128641.

Velusamy, S., Sakthivel, S., Sangwai, J.S., 2017. Effect of imidazolium-based ionic liquids on the interfacial tension of the alkane-water system and its influence on the wettability alteration of quartz under saline conditions through contact angle measurements. Ind. Eng. Chem. Res. 56, 13521–13534.

Wang, L., Liu, J., Huo, S., et al., 2014a. Synthesis and surface properties of novel gemini imidazolium surfactants. J. Surfactants Deterg. 17 (6), 1107–1116. https://doi.org/10.1007/s11743-014-1615-0.

Wang, L., Qin, H., Ding, L., et al., 2014b. Preparation of a novel class of cationic gemini imidazolium surfactants containing amide groups as the spacer: their

surface properties and antimicrobial activity. J. Surfactants Deterg. 17 (6), 1099–1106. https://doi.org/10.1007/s11743-014-1614-1.
Wu, L., Liao, L., Lv, G., et al., 2014. Microstructure and process of intercalation of imidazolium ionic liquids into montmorillonite. Chem. Eng. J. 236, 306–313. https://doi.org/10.1016/j.cej.2013.09.063.
Wu, N., Wu, L., Liao, L., et al., 2015. Organic intercalation of structure modified vermiculite. J. Colloid Interface Sci. 457, 264–271. https://doi.org/10.1016/j.jcis.2015.07.031.
Xiang, Y., Gao, M.L., Ding, F., et al., 2019a. The efficient removal of dimethyl phthalate by three organo-vermiculites with imidazolium-based gemini surfactants in aqueous media. Colloids Surf. A Physicochem. Eng. Asp. 580, 123726. https://doi.org/10.1016/j.colsurfa.2019.123726.
Xiang, Y., Gao, M.L., Shen, T., et al., 2019b. Comparative study of three novel organo-clays modified with imidazolium-based gemini surfactant on adsorption for bromophenol blue. J. Mol. Liq. 286, 110928. https://doi.org/10.1016/j.molliq.2019.110928.
Xie, G., Xiao, Y., Deng, M., et al., 2020. Investigation on the inhibition mechanism of alkyl diammonium as montmorillonite swelling inhibitor: experimental and molecular dynamics simulations. Fuel 282, 118841. https://doi.org/10.1016/j.fuel.2020.118841.
Xin, X., Si, W., Yao, Z., et al., 2011. Adsorption of benzoic acid from aqueous solution by three kinds of modified bentonites. J. Colloid Interface Sci. 359 (2), 499–504. https://doi.org/10.1016/j.jcis.2011.04.044.
Yin, X., Wang, X., Wu, H., et al., 2017. Enhanced desorption of cesium from collapsed interlayer regions in vermiculite by hydrothermal treatment with divalent cations. J. Hazard Mater. 326, 47–53. https://doi.org/10.1016/j.jhazmat.2016.12.017.
Yu, S., Pang, H., Huang, S., et al., 2021. Recent advances in metal-organic framework membranes for water treatment: a review. Sci. Total Environ. 800, 149662. https://doi.org/10.1016/j.scitotenv.2021.149662.
Yuan, S., Gu, J., Zheng, Y., et al., 2015. Purification of phenol-contaminated water by adsorption with quaternized poly(dimethylaminopropyl methacrylamide)-grafted PVBC microspheres. J. Mater. Chem. 3 (8), 4620–4636. https://doi.org/10.1039/C4TA06363E.
Zeng, H., Gao, M.L., Shen, T., et al., 2018. Organo silica nanosheets with gemini surfactants for rapid adsorption of ibuprofen from aqueous solutions. J. Taiwan Inst. Chem. Eng. 93, 329–335. https://doi.org/10.1016/j.jtice.2018.07.038.
Zhang, H., Li, M., Yang, B., 2018. Design, synthesis, and analysis of thermophysical properties for imidazolium-based geminal dicationic ionic liquids. J. Phys. Chem. C 122 (5), 2467–2474. https://doi.org/10.1021/acs.jpcc.7b09315.
Zhang, S., Wang, J., Zhang, Y., et al., 2021. Applications of water-stable metal-organic frameworks in the removal of water pollutants: a review. Environ. Pollut. 291, 118076. https://doi.org/10.1016/j.envpol.2021.118076.
Zhou, L., Chen, H., Jiang, X., et al., 2009. Modification of montmorillonite surfaces using a novel class of cationic gemini surfactants. J. Colloid Interface Sci. 332 (1), 16–21. https://doi.org/10.1016/j.jcis.2008.12.051.
Zhou, L., He, Y., Gou, S., et al., 2020. Efficient inhibition of montmorillonite swelling through controlling flexibly structure of piperazine-based polyether Gemini quaternary ammonium salts. Chem. Eng. J. 383, 123190. https://doi.org/10.1016/j.cej.2019.123190.